sustainability

IMPACT FACTOR 3.3

CITESCORE 6.8

Article

# Characterization of Stone Waste Sludge and Preliminary Investigation on Green Materials Based on Traditional Lime Putty for Sustainable Construction

Albina Scioti, Graziella Bernardo, Ippolita Mecca and Fabio Fatiguso

Special Issue

Innovative Approaches, Techniques and Technologies Related to Retrofitting Architectural Heritage for Sustainable and Resilient Cities

Edited by
Dr. Elena Cantatore

MDPI

https://doi.org/10.3390/su16219173

*sustainability*

MDPI

*Article*

# Characterization of Stone Waste Sludge and Preliminary Investigation on Green Materials Based on Traditional Lime Putty for Sustainable Construction

**Albina Scioti [1], Graziella Bernardo [2], Ippolita Mecca [3] and Fabio Fatiguso [1,*]**

[1] DICATECh Department, Polytechnic of Bari, Via Orabona, 4, 70125 Bari, Italy; albina.scioti@poliba.it
[2] Department of European and Mediterranean Cultures, Basilicata University, 85100 Potenza, Italy; graziella.bernardo@unibas.it
[3] D-ENG Department, Faculty of Engineering and Informatics, Pegaso Telematic University, 80132 Napoli, Italy; ippolita.mecca@unipegaso.it
* Correspondence: fabio.fatiguso@poliba.it

**Abstract:** Very large quantities of stone waste sludge are disposed in exhausted quarries and have a very low reuse rate to date. The paper considers the possibility of using these types of industrial waste in partial substitution of natural aggregates for the production of lime-based plasters. Traditional materials based on lime, the only material with a carbon neutrality life cycle, have considerable potential for use as components of green materials for plastering and finishing building surfaces in both new construction and historic heritage conservation. The paper presents the preliminary results of a research activity aimed at developing pre-packaged products based on Traditional Lime Putty (TLP) by partially replacing natural aggregates with Stone Waste Sludge (SWS), with a low rate of recovery from the Apricena limestone production district in Apulia. The mineralogical and chemical analysis carried out using XRD (X-Ray Diffraction), TG-DTA (Thermo Gravimetry-Differential Thermal Analysis), and hydrochloric acid attack test showed that the SWS consisted of 98.4 % $CaCO_3$ by mass. The particle sizes measured by laser diffraction technique are below 22.5 µm for the 92% mass of the sample. The high fineness of the stone waste was confirmed by the Blaine-specific surface method, which equals to 9273.79 $cm^2$/gr. The behavior of three fresh mixtures for prepacked coarse plaster, fine plaster, and finishing plaster with 12.90%, 17.94%, and 18.90 by mass of SWS, respectively, was evaluated by spreading test and applicability tests on a perforated ceramic slab. The finishing plaster has the highest consistency value of 235 mm, while the fine plaster and the coarse plaster have values of 205 mm and 155 mm, respectively. The coarse plaster is suitable for use as base plaster (arriccio) or second layer rendering (tonachino) up to a thickness of approximately 1 cm. Both the fine plaster and finishing plasters can be used for the surfaces finishing with the application of layers of a few millimeters thick.

**Keywords:** waste recycling; stone waste sludge; waste reduction; traditional lime putty; sustainable materials



**Citation:** Scioti, A.; Bernardo, G.; Mecca, I.; Fatiguso, F. Characterization of Stone Waste Sludge and Preliminary Investigation on Green Materials Based on Traditional Lime Putty for Sustainable Construction. *Sustainability* **2024**, *16*, 9173. https://doi.org/10.3390/su16219173

Academic Editor: Ning Yuan

Received: 5 August 2024
Revised: 1 October 2024
Accepted: 21 October 2024
Published: 22 October 2024



## 1. Introduction

In recent years, there has been a growing interest in lime-based materials used for the preparation of mortars, plasters, and paints in water solutions. In the field of the conservation of the built heritage, lime-based products show the requirements of physical, chemical, and mechanical compatibility with vertical closures typically made of stone or brick [1–4]. Furthermore, lime is a material that can greatly contribute to the fight against climate change by reducing the amount of carbon dioxide released into the atmosphere [5–8]. The so-called lime cycle involving limestone burning, slaking of quicklime (CaO), and carbonation of calcium hydroxide ($Ca(OH)_2$) offers the environmental benefit of carbon neutrality that the same amount of carbon dioxide emitted by limestone calcination is captured during

the phase of hardening. For this reason, there is a rediscovery of lime-based materials in the new construction sector as well. Their use can contribute significantly to the ecological transition of the construction sector. Moreover, the lime-based surface finishings have a high biocidal power thanks to the high alkalinity and guarantee the conditions of environmental comfort for their high vapor breathability. Numerous studies have shown that the traditional production processes using wood as fuel with a calcination temperature around 800–1000 °C and the aging of lime putty give a lime of better quality with a high reactivity of the particles of calcium hydroxide [9–17]. Lime putties obtained traditionally and aged for a long period according to the good practices handed down by Vitruvio show the presence of nanosized particles ranging from 50 to 130 nanometers [14,15]. The nanometric dimensions of traditional slaked lime with a high specific surface area and high reactivity justify the excellent technological properties and high durability of Roman concrete made from mixtures of long-aging slaked lime and pozzolan. Therefore, the use of Traditional Lime Putty (TLP) can lead to the development of high-performance nanotechnological green materials with a wide range of applications both in the conservation of the built heritage and in new buildings [18]. Moreover, the sustainability of traditional lime products can be increased by replacing natural or artificial aggregates with waste or scrap from other production processes.

Fine dust from the quarrying and processing of ornamental stones is potentially suitable for reuse as an inert component of new green materials designed to reduce the amount of waste taken to landfills.

Preceded by China, India, Turkey, Iran, and Brazil, in 2018, Italy ranked sixth as a producer of stone materials worldwide, with volumes totaling 6 million tons, accounting for almost 4% of the market share [19]. The extraction and processing of stone involve two primary mechanical treatments, namely the ashlar-size cutting and the surface grinding-polishing. These mechanical operations generate a considerable amount of various types of waste having the same chemical composition but different sizes. The stone wastes can be categorized into two types: (i) large scraps and debris, and (ii) sawdust sludge with a solid content of less than 10 percent in mass. This latter one is produced by using water for lubrication, cooling of tools with diamond blades, and dust abatement in workplaces. Sawdust sludge undergoes an initial sedimentation process, raising the percentage of solid matter to 30–35% with the recovery of the aqueous fraction in the production cycle. The subsequent process of filter pressing increases the content of solid matter up to 70–75% and originates a waste, known as marmettola (SWS), which is taken to a landfill or used to fill decommissioned quarries.

The waste generated from the cutting and processing of stone can range from a minimum of 35% to a maximum of 75% of the stone product. Thus, from 100 kg of stone (block) input, only 25 kg of finished product can be obtained, while the remaining 75 kg is waste. On average, the SWS is equal to 22.5% of the processed raw material. In Italy, the ISTAT data for "Extractions of non-energy mineral resources from quarries and mines by type, region, and geographic distribution" in 2020 [20] reports an annual production of extracted stone materials of 98,587,000 tons, which implies the production of SWS in the same year amounting to 22,182,000 tons. In the same year, Apulia (Puglia) and Basilicata extracted 13,074,000 tons and 3,252,000 tons of product, respectively, with a corresponding production of approximately 2,942,000 tons and 732,000 tons of SWS.

According to Italian regulations, SWS is subject to waste provisions and must be classified under the code "CER 01 04 13—waste produced from stone processing, different from those referred to in item 01 04 07". There is the possibility of being classified as a by-product when it can be used in other processing cycles and meets all the requirements of Article 184 bis of Legislative Decree 152/2006. In the absence of even one of the conditions provided by the regulation, the material remains classified as waste with code "CER 01 04 13" and must be disposed of, obligatorily, according to the SISTRI system, in authorized landfills in the ways prescribed by the Environmental Code if it is not recycled [21].

Many studies explore the reuse of SWS in various industrial contexts within the engineering field. For instance, one potential application involves using SWS as a neutralizing agent for acidic wastewater in the glass industry [22] or as a heavy metal removal on industrial wastewater [23]. Due to its finely reduced granularity, the SWS is expected to expedite and simplify the limestone suspension process required for neutralization. Additionally, it finds application in the desulfurization of combustion fumes in high-power industrial burners, utilizing both dry and wet technologies [24–26]. Moreover, SWS can be employed as a soil amendment for neutralizing acidic agricultural soils, enhancing their performance by raising the pH and impeding water evaporation through its significant hygroscopic properties [27,28]. In the realm of the construction industry, numerous studies highlight the utilization of stone processing waste as a secondary raw material in formulating innovative materials for the production of concrete [29–43], bricks [44], cement [45–47], tiles [48], and mortar [49–58]. SWS can replace cement and/or fine aggregate with different percentages due to its high fineness, which provides good cohesiveness of the mix, increases the workability, and reduces the permeability of concrete. To increase the cement-based mortar's workability, lime is added in substitution of part of the cement, so in some studies, the replacement of the hydrated lime with SWS is tested [55]. In other studies, the replacement of part of sand with SWS is tested both in cement and lime-based mortars [56] and in only lime-based mortars [57]. In addition, further research revealed the opportunity to use marble slurry as a binder to produce a calcitic air-hardening lime [58].

The paper presents the preliminary results of a research activity aimed at developing TLP-based green materials, such as mortars and plasters, by partial substitution of natural aggregates with stone processing waste, called SWS, from the Apricena limestone production district in Apulia. The innovativeness of the research lies in the fact that, as mentioned, this application is to date not much investigated in science. Preliminary studies therefore concern the characterization of SWS, the design of the mixtures, and initial verifications of the behavior in the fresh state of the proposed mixtures.

## 2. Materials and Methods

### *2.1. Materials*

TLP with an aging period of six months produced by Legnami Adriatica of Fasano (Brindisi, Apulia, Italy) was used for the preparation of the mixtures of green mortar and plaster. The company was founded in 1945 as a timber production company for the building and carpentry industry. A few years after its foundation, the wood-fired lime production line was added to the industrial carpentry activity to recover as a source of energy the large quantities of wood residues resulting from the debarking and sawing of wood logs.

Figure 1a shows the production kilns of the vertical type with four natural draught side fireplaces and automatic lifting skips for loading limestone pebbles from the top. Kilns use wood production waste as fuel and reach temperatures of 900–1000 °C. The limestone pebbles descend into the kiln, encountering increasingly hot fumes in counterflow. In this way, a gradually fired, fat, white, and pure quicklime is produced. The quicklime is slaked in tanks where long-term aging of lime putty also takes place (Figure 1b).

Three different types of ground calcareous sand were used for sample preparation: (1) coarse sand with a maximum diameter of 3 mm; (2) fine sand with a maximum diameter of 2 mm; (3) fine white sand with a maximum diameter of 1 mm obtained from the Carovigno limestone.

The selected aggregates are usually used for the preparation of commercial premixed products of the company.

The stone waste was taken from the San Sabino landfill in Apricena. Apricena stone comes from the extraction and processing of carbonate rock in quarries located near the town of Apricena, from which it takes its name. It is a white stone material belonging to the local construction tradition that is still widely used in the building industry and that generates a large amount of waste with a low rate of recovery. In 2022, in the extraction district of Apricena, a total of 17,800 tons of SWS were disposed of in the quarry.

(**a**) (**b**)

**Figure 1.** (**a**) Vertical kilns for the production of quicklime; (**b**) Tanks of quicklime slaking and long-term aging of lime putty.

Figure 2 shows the tool with a water-cooled diamond blade used in the cutting and processing of the limestone rock. The sawing sludge is first subjected to sedimentation in a settler and then filter-pressed. Figure 3a,b illustrate, respectively, the filter-pressing system filter and the stone waste, SWS, at the end of treatment. A polyelectrolyte solution (flocculant) is added to sawdust sludge with a dosage of 70–80 mg per 1 kg of dry material before entering the settler to enhance the settling speed of solid particles. The cutting of 1 $m^2$ of stone requires an average of 10 L/min of water and produces around 18.5 kg of filter-pressed SWS. The collected SWS is transported to landfills for inert materials, typically located in decommissioned quarries, and utilized until their filling (Figure 4).

**Figure 2.** The tool with a water-cooled diamond blade during the processing of Apricena limestone block.

(**a**) (**b**)

**Figure 3.** (**a**) Filter-pressing system; (**b**) SWS at the end of the filter-pressing operations.

**Figure 4.** SWS—San Sabino landfill in Apricena (FG), Italy.

*2.2. Analytical Techniques for Mineralogical, Chemical, and Physical Characterization of Apricena SWS*

The mineralogical and chemical characterization of the SWS was carried out using the X-ray diffraction (XRD) technique and thermogravimetry differential thermal analysis (TG-DTA). A powder diffractometer, Philips PW 3710 (Almelo, The Netherlands), with monochromatic CuK $\alpha$ radiation ($\lambda$ = 0.154056 nm) at 40 kV and 30 mA was used for the identification of mineralogical phases. The diffraction data were collected from 0 to 60° of 2$\theta$ at a scan rate of 2° 2$\theta$ per minute. A simultaneous thermal analyzer, Netzsch STA 400 (Selb, Germany), equipped with a computerized data processing system was used for TG-DTA. The heating test was performed at the maximum temperature of 1100 °C with a fixed rate of 10 °C/minute in static air. The value of non-carbonate impurities was also verified by acid attack of the sample with a 3% solution of hydrochloric acid and subsequent filtration of the solution with a paper filter.

The chemical composition of SWS was determined by X-ray fluorescence spectrometry using a Siemens SRS 303 sequential spectrometer (Karlsruhe, Germany).

To verify the non-hazardous classification of the SWS, according to the reference standard, it was subjected to an eluate analysis according to UNI 10802:2023. [59]

The specific weight of the sample was calculated using a pycnometer Labortech 2000 LLG04008329 (Milan, Italy) with a wide neck and distilled water.

The sample's moisture content was calculated through successive measurements of the mass of a sample heated in a ventilated oven at a temperature of 110 °C until a constant mass value was reached.

The ISO test was also performed to evaluate the Brightness [60,61].

The particle size distribution of SWS was evaluated using the sedimentation method of liquid dispersions of samples in demineralized water. In addition, considering the fineness of the sawdust sludge, the laser diffraction method with Mastersize-S equipment from Malvern Instruments (Malvern, UK) was employed to measure the particle sizes of stone waste. The technique is based on the principle that particles illuminated by a laser beam scatter light at an angle related to their size. As the particle size decreases, the observed angle of scattering (diffusion) increases logarithmically.

The specific surface of the SWS was also assessed using the Blaine Method according to UNI EN 196-6:2019 [62]. The equipment used is a Blaine's Air Permeameter from Controls Srl, model 62-L0042/A. Under normalized conditions, the specific surface area of the sample is directly proportional to $\sqrt{t}$, where t is the time required for a certain amount of air to pass through the sample. To calibrate the instrument, a Portland cement with the specific weight $\rho o$ = 3.15 [g/cm$^3$], $\sqrt{to}$ = 9.92 [s$^{1/2}$], specific surface area So = 3774 [cm$^2$/g].

*2.3. Preparation of Mortars and Plasters Based on TLP and SWS*

For the preparation of mortar and plaster samples, an analytical balance, volumetric dosing containers, and a propeller stainless mixer were used.

The behavior of three types of fresh plasters based on TLP and stone waste has been evaluated. The first mixture is a coarse plaster containing 6 parts in volume of coarse sand ($d_{max}$ = 3 mm) and 1 part in volume of SWS with a volume ratio of aggregate and lime putty of 3.5. The second mixture is a fine plaster containing 6 parts in volume of sand ($d_{max}$ = 2 mm) and 1 part in volume of SWS with a volume ratio of aggregate and lime putty of 3.5. The third mixture is a finishing plaster containing 2 parts in volume of white fine sand ($d_{max}$ = 1 mm) and 0.5 part in volume of SWS with a volume ratio of aggregate and lime putty of 2.5, as shown in Table 1.

**Table 1.** Aggregate components and volume ratio of aggregate and lime putty of the tested mixtures.

| Type of Plaster | AC [1] | PV [1] | VRALP [1] |
|---|---|---|---|
| Coarse Plaster | SWS<br>CS [2] | 1<br>6 | 3.5 |
| Fine Plaster | SWS<br>FS [2] | 1<br>6 | 3.5 |
| Finishing Plaster | SWS<br>WFS [2] | 0.5<br>2 | 2.5 |

[1] AC = Aggregate Component; PV = Parts in Volume; VRALP = volume ratio of aggregate and lime putty. [2] CS = Coarse Sand ($d_{max}$ = 3 mm); FS = Fine Sand ($d_{max}$ = 2 mm); WFS = White Fine Sand ($d_{max}$ = 1 mm).

Table 2 shows the bulk density of the mixtures' components measured using the weight of the dried samples contained in a graduated transparent cylinder of 200 cc. Table 3 shows the composition in parts by volume and by mass of the mixtures.

**Table 2.** Bulk density of the components of the tested mixtures.

| Component | M [1] | BD [1] |
|---|---|---|
| | g | g/cm$^3$ |
| TLP | 26 | 509.54 |
| SWS | 26 | 507.56 |
| CS [2] | 26 | 500.27 |
| FS [2] | 26 | 449.35 |
| WFS [2] | 26 | 420.00 |

[1] M = mass; BD = bulk density. [2] CS = Coarse Sand ($d_{max}$ = 3 mm); FS = Fine Sand ($d_{max}$ = 2 mm); WFS = White Fine Sand ($d_{max}$ = 1 mm).

**Table 3.** Composition in parts by volume and by mass of the tested mixtures.

| Type of Plaster | Component | PV | M [1] | %M [1] |
|---|---|---|---|---|
| | | | kg | g/cm$^3$ |
| Coarse Plaster | TLP | 2 | 0.468 | 17.75 |
| | SWS | 1 | 0.340 | 12.90 |
| | CS [2] | 6 | 1.728 | 65.55 |
| | W [2] | 0.5 | 0.100 | 3.80 |
| Fine Plaster | TLP | 2 | 0.468 | 24.70 |
| | SWS | 1 | 0.340 | 17.94 |
| | FS [2] | 6 | 0.987 | 52.08 |
| | W [2] | 0.5 | 0.100 | 5.28 |
| Finishing Plaster | TLP | 1 | 0.234 | 25.11 |
| | SWS | 0.5 | 0.170 | 18.24 |
| | WFS [2] | 2 | 0.428 | 45.92 |
| | W [2] | 0.5 | 0.100 | 10.73 |

[1] PV = Parts in Volume; M = mass; %M = % in mass. [2] CS = Coarse Sand ($d_{max}$ = 3 mm); FS = Fine Sand ($d_{max}$ = 2 mm); WFS = White Fine Sand ($d_{max}$ = 1 mm).

The masses of the components were obtained by multiplying the bulk density by the volume parts of the mix design. The mass percentages of the components were obtained from the total mass of the mixtures. The dosages of SWS in the coarse plaster, fine plaster, and finishing plaster are equal, respectively, to 12.90% in mass of total mix and 16.44% in mass of aggregate, 17.94% in mass of total mix, and 25.62% in mass of aggregate, 18.24% in mass of total mix, and 28.42% in mass of aggregate. A 2.25 kg sample was prepared for each mixture.

The mixtures were prepared according to volumetric dosages in accordance with the usual practice of the industry where the trials were carried out, with volumetric ratios of aggregate to plaster of 3.5 for coarse and fine plaster and 2.5 for finishing plaster. The percentage substitution of natural aggregates for waste was also based on the company's practice in preparing similar mixtures using artificial aggregates obtained from demolition waste of similar fineness.

Figure 5 shows the appearance after mixing the three samples of coarse plaster, fine plaster, and finishing. For each sample, a mass of 900 g was used for consistency measurement with the spreading test. The remaining quantity was used for the applicability tests on perforated brick. The consistencies of the mortars are different from each other as the aggregates used are of decreasing grain size, starting with the coarse mortar and ending with the finishing plaster.

(**a**) (**b**) (**c**)

**Figure 5.** Samples of coarse mortar (**a**), fine plaster (**b**) and finishing plaster (**c**) after mixing.

The consistency of the samples was evaluated with the spreading test according to UNI EN 1015-3:2007 [63]. The equipment used to perform this test consists of a shake table with a drop height of 15 mm with a frequency of 60 drops per minute and a truncated cone mold in stainless steel with a height of 60 mm and diameters of 100 mm and 70 mm and a thickness of 2 mm. The test was performed on a sample of approximately 900 g of fresh mortar placed inside the truncated cone mold in two layers, each of which was compacted by at least 10 short pestle strokes to ensure an even filling of the mold. After about 15 s, the mold was slowly lifted vertically, and the mortar was spread on the disk by vibrating the flow table 15 times at a constant frequency of about one blow per second. The diameter of the mortar in two mutually perpendicular directions was measured using a gauge. The average value of the two measurements is the consistency value of the test sample.

Plaster applicability tests were carried out on a ceramic slab using metal and wooden trowels.

## 3. Results and Discussion

### *3.1. Characterization of Apricena Stone Waste (SWS)*

A 5 kg sample was taken and brought to the laboratory for the necessary characterization tests. After suitable homogenization with a mixer, different amounts were taken from this sample for the different tests.

Mineralogical analysis was carried out by X-ray diffractometry. Figure 6 shows the diffraction pattern of the fine powder sample. The X-ray pattern was compared with the

Jade Library Joint Committee on Powder Diffraction Standards (JCPDS) card. Results show that the main phase is calcite ($CaCO_3$), Dolomite ($MgCa(CO_3)$) and hematite ($\alpha$- $Fe_2O_3$) were detected as compounds in traces.

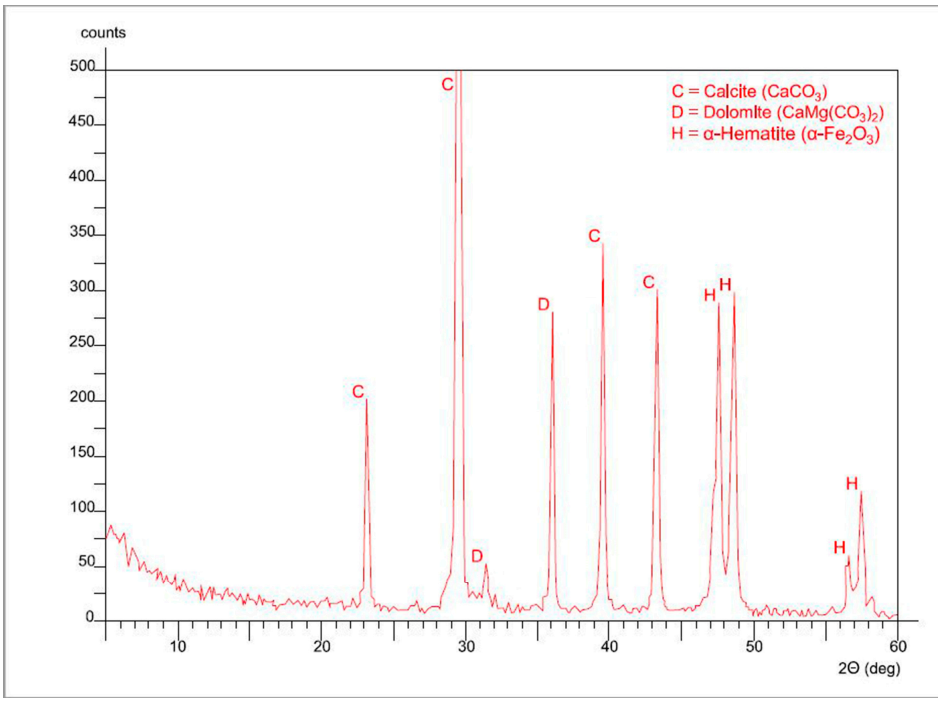


**Figure 6.** X-ray diffraction pattern of the fine powder sample.

Figure 7 illustrates the results of TG-DTA. The differential temperature curve shows an endothermic peak at the temperature of 900 °C at which the calcination reaction takes place with the formation of calcium oxide and the release of carbon dioxide [64,65], according to the following Equation (1):

$$CaCO_3 \rightarrow CaO + CO_2 \quad (1)$$

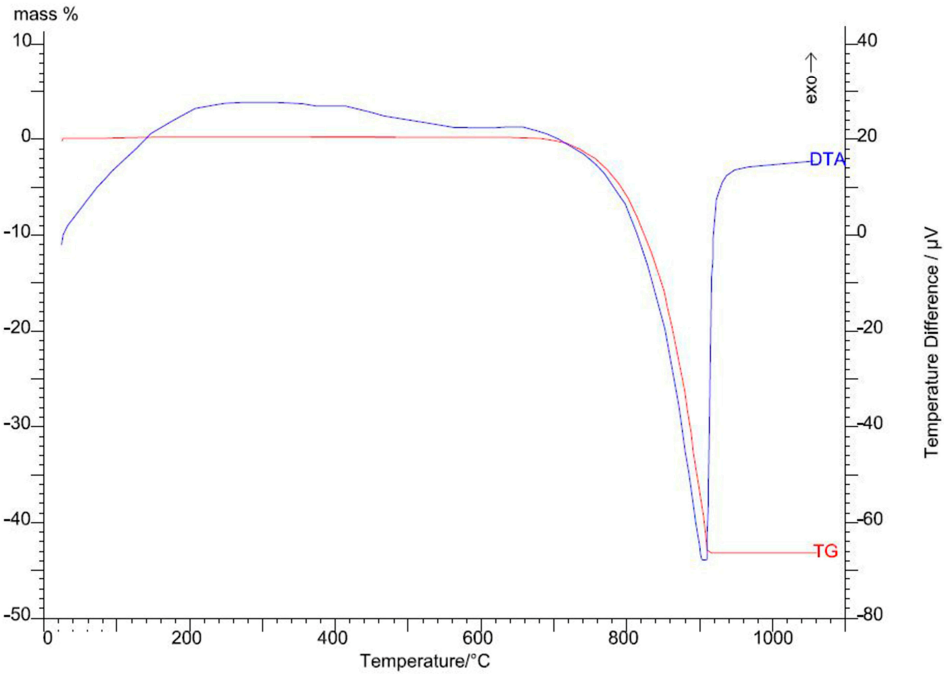


**Figure 7.** Thermogravimetric and differential thermal curves of SWS.

The thermogravimetric curve shows a sample mass loss of 43.30%. This value is below the stoichiometric mass loss equal to 44% of the calcination reaction. It indicates a calcium carbonate content of 98.41% by mass. The experimental data were confirmed by the hydrochloric acid attack performed on two powder samples.

The results of the hydrochloric acid attack test on SWS samples to verify the presence of impurities, shown in Table 4, indicate an average value of non-carbonate impurities of 1.56% by mass and a calcium carbonate content equal to 98.44% by mass, which is in agreement with the experimental data obtained by TG-DTA. The nature of non-carbonated impurities in the sample can be investigated through further chemical analyses, but given the insignificance of the percentage, no further investigation was deemed necessary at this stage.

**Table 4.** Hydrochloric acid attack test on samples of SWS

| Sample Code | M [1] g | IMPF [1] g | FMPF [1] g | NCI [1] g | %M [1] % | AVM [1] % | σ |
|---|---|---|---|---|---|---|---|
| S1 | 9.9225 | 1.1932 | 1.3672 | 0.1740 | 1.7535 | 1.5592 | 0.01 |
| S2 | 9.9340 | 1.1695 | 1.3051 | 0.1356 | 1.3650 | | |

[1] M = Mass; IMPF = Initial mass of paper filter; FMPF = Final mass of paper filter; NCI = Non-carbonate impurities; %M = % in mass; AVM = Average value, % in mass.

The chemical composition of SWS was determined by X-ray fluorescence spectrometry to support the XRD analysis carried out quantitatively. The results are presented in Table 5. SWS is composed mainly of CaO, consistent with what has been observed in the other characterization tests. All other components are present in amounts less than 0.1% except MgO.

**Table 5.** Chemical composition on SWS samples

| Sample Code | $Fe_2O_3$ % | $Al_2O_3$ % | $SiO_2$ % | CaO % | MgO % | $Na_2O$ % | $K_2O$ % | $TiO_2$ % | $SO_4$ % | $CO_2$ % |
|---|---|---|---|---|---|---|---|---|---|---|
| S3 | 0.04 | 0.06 | 0.01 | 55.60 | 0.25 | 0.015 | 0.024 | 0.02 | 0.03 | 43.95 |
| S4 | 0.03 | 0.08 | 0.02 | 55.54 | 0.24 | 0.013 | 0.025 | 0.03 | 0.04 | 43.28 |

The results of the eluate analysis, aimed at verifying the presence or absence of hazardous elements within the SWS, are shown in Table 6. In relation to these results and with reference to the Italian Regulations [66], the SWS is found not to be "non-hazardous waste" and can be destined for recovery.

**Table 6.** Eluate analysis on SWS samples.

| Component | S5 | S6 |
|---|---|---|
| pH [4] | 8.7 | 8.7 |
| COD [1] | 15.8 mg/L | 12.8 mg/L |
| As | NRIB [2] $x_1$ [3] | NRIB [2] $x_1$ [3] |
| Ba | NRIB [2] $x_2$ [3] | NRIB [2] $x_2$ [3] |
| Be | NRIB [2] $x_1$ [3] | NRIB [2] $x_1$ [3] |
| Cd | NRIB [2] $x_1$ [3] | NRIB [2] $x_1$ [3] |
| Co | NRIB [2] $x_3$ [3] | NRIB [2] $x_3$ [3] |
| Cr | NRIB [2] $x_1$ [3] | NRIB [2] $x_1$ [3] |
| Hg | NRIB [2] $x_1$ [3] | NRIB [2] $x_1$ [3] |
| Ni | NRIB [2] $x_1$ [3] | NRIB [2] $x_1$ [3] |
| Pb | NRIB [2] $x_1$ [3] | NRIB [2] $x_1$ [3] |
| Cu | NRIB [2] $x_4$ [3] | NRIB [2] $x_4$ [3] |
| Se | NRIB [2] $x_1$ [3] | NRIB [2] $x_1$ [3] |

**Table 6.** *Cont.*

| Component | S5 | S6 |
|---|---|---|
| V | 7.3 µg/L | 6.2 µg/L |
| Zn | NRIB [2] $x_2$ [3] | NRIB [2] $x_2$ [3] |
| Nitrates | 0.4 mg/L | NRIB [2] $x_2$ [3] |
| Chlorides | 47.9 mg/L | 2.3 mg/L |
| Fluorides | NRIB [2] $x_5$ [3] | NRIB [2] $x_5$ [3] |
| Sulfates | 58.2 mg/L | NRIB [2] $x_6$ [3] |
| Cyanides | NRIB [2] $x_1$ [3] | NRIB [2] $x_1$ [3] |

[1] COD = chemical oxygen demand. [2] NRIB = not relevant if below threshold x. [3] $x_1$ = 0.1 µg/L; $x_2$ = 0.1 mg/L; $x_3$ = 0.001 mg/L; $x_4$ = 0.01 mg/L; $x_5$ = 0.5 mg/L; $x_6$ = 1.0 mg/L; [4] pH limit values < 5.5 and >12.

The specific gravity measured with the use of a pycnometer and an analytical balance gave the value of 2.80 g/cm$^3$.

The moisture content of the SWS was measured by using a ventilated oven and an analytical balance was equal to 23.5%.

The test conducted to measure the ISO Brightness Level indicated a very high and nearly pure degree of whiteness with a value of 93.5% ± 1.

Table 7 illustrates the particle size distribution of solid particles obtained by the method of sedimentation of liquid dispersions in the water of the sample of SWS. According to the AGI Classification [67], it can be defined as weakly sandy and clayey silt.

**Table 7.** Particle size distributions by sedimentation of liquid dispersion of the sample of SWS.

| Component | d [1] | %M [1] | σ |
|---|---|---|---|
| | µm | % | |
| Clay | d < 2 | 10 | 0.11 |
| Silt | 2 < d < 20 | 75 | 1.33 |
| Sand | d > 20 | 15 | 0.73 |

[1] d = diameter; %M = % in mass.

Figure 8 shows the particle distribution obtained by the laser diffraction method. The maximum particle size, expressed as equivalent diameter, is equal to 77 µm. It can be observed that only 8% in mass have a particle size ranging between 22.5 µm and 77 µm, while the remaining 92% in mass have a particle size below 22.5 µm, with 7% in mass having a particle size below 0.5 µm.

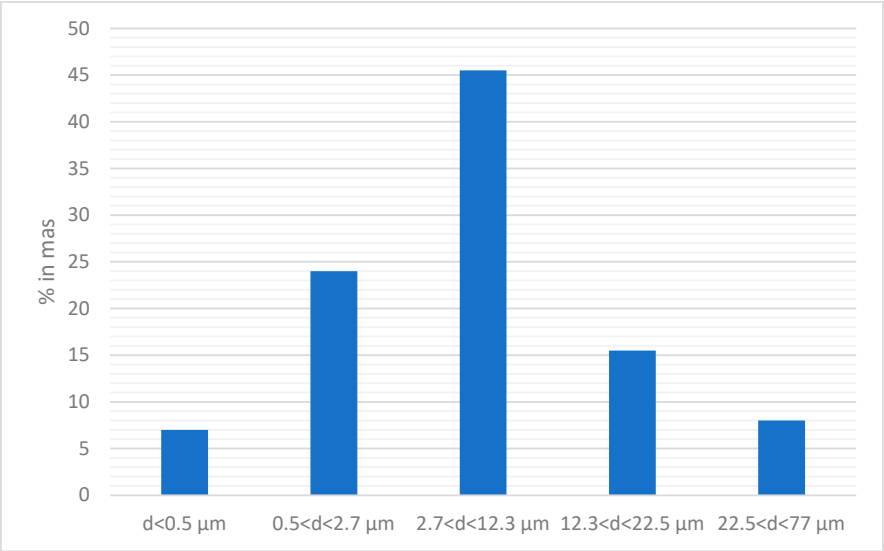


**Figure 8.** Particle size distribution obtained by laser diffractometry test.

Five measurements were performed to calculate the specific surface area using the Blaine method: A1, A2, and A3 on the same sample, and B1 and B2 on a different sample. For each measurement, the temperature, measurement time and the time t taken for the air to pass through the sample were recorded. The specific surface area of each sample was calculated using the following Formula (2):

$$S_i = K\sqrt{t} \quad (2)$$

where the constant K is equal to 1198.40 [$cm^{-1} \cdot s^{-1/2}$] using the following Formula (3):

$$K = \frac{\rho_o}{\rho} \frac{S_o}{\sqrt{t_o}} \quad (3)$$

with

- ρo = 3.15 [$g/cm^3$], specific weight of Portland cement
- ρ = 2.80 [$g/cm^3$], specific weight of SWS
- So = 3.774 [$cm^2/g$], specific surface area of Portland cement
- $\sqrt{to}$ = 9.92 [$s^{1/2}$], time required for the air passage through the Portland cement sample used for the equipment's calibration.

Table 8 shows the experimental data of Blaine specific surface area values obtained by the Blaine method. The specific surface obtained by the overall average value over the five samples is 9273.79 $cm^2/g$. This value confirms the significant fineness of the SWS.

**Table 8.** Experimental data of Blaine-specific surfaces of SWS samples.

| Sample Code | T [1] | t [1] | √t | BSS [1] | σ |
|---|---|---|---|---|---|
| | °C | s | $s^{-1/2}$ | $cm^2/g$ | |
| A1 | 26 | 509.54 | 22.57 | 9661.24 | 46.51 |
| A2 | 26 | 507.56 | 22.53 | 9642.45 | |
| A3 | 26 | 500.27 | 22.37 | 9572.95 | |
| B1 | 26 | 449.35 | 21.20 | 9072.69 | 213.05 |
| B2 | 26 | 420.00 | 20.49 | 8771.39 | |

[1] T = temperature; t = time; BSS = Blaine-Specific Surface.

### *3.2. Evaluation of Fresh Plasters' Behavior*

In regard to the particular research that examines the preparation of plasters and finishes, the behavior in the fresh state is of paramount importance, as these are materials that are primarily dependent on good workability and applicability. The workability of the materials was therefore evaluated through the use of spreading tests. Figure 9 shows the samples of coarse mortar, fine plaster, and finishing plaster after the mold lift during the spreading test.

(**a**) (**b**) (**c**)

**Figure 9.** Samples of coarse mortar (**a**), fine plaster (**b**) and finishing plaster (**c**) after the mold lift during the spreading test.

Table 9 shows the values of the two orthogonal diameters measured with a gauge and the average value of the two measurements. The latter value indicates the consistency of the mixtures. The finishing plaster has the highest consistency value of 235 mm. Fine plaster has a consistency of 205 mm, while coarse plaster has a value of 155 mm. These results are consistent with other studies on the fresh state of mortar [68,69], and fall into the typical range of commercial products packaged with natural aggregates and not contemplating the use of recycled materials

**Table 9.** Measurements of spread diameters

| Type of Plaster | d [1] mm | Cd [1] mm | Md [1] mm | σ |
|---|---|---|---|---|
| Coarse Plaster | 150 | 160 | 155 | 4.12 |
| Fine Plaster | 200 | 210 | 205 | 4.00 |
| Finishing Plaster | 240 | 230 | 235 | 3.81 |

[1] d = diameter; Cd = Cross diameter; Md = Mean diameter.

Figures 10–12 show the applicability tests of coarse mortar, fine plaster, and finishing plaster, respectively. The sample of coarse mortar was applied on the surface of a perforated ceramic slab, previously impregnated with water applied with a brush. The first layer of 0.5 cm was applied using a steel trowel. The second layer of 0.5 was applied when the surface began to harden (whereby no more marks were left by touching the surface). Finally, before the second coat was completely dry, the surface was worked over with the wooden trowel with circular movements that allowed it to drag the larger granules of aggregate and give rise to small grooves on the surface. The roughness of the surfaces obtained in this way of application ensures good adhesion of the subsequent layers.

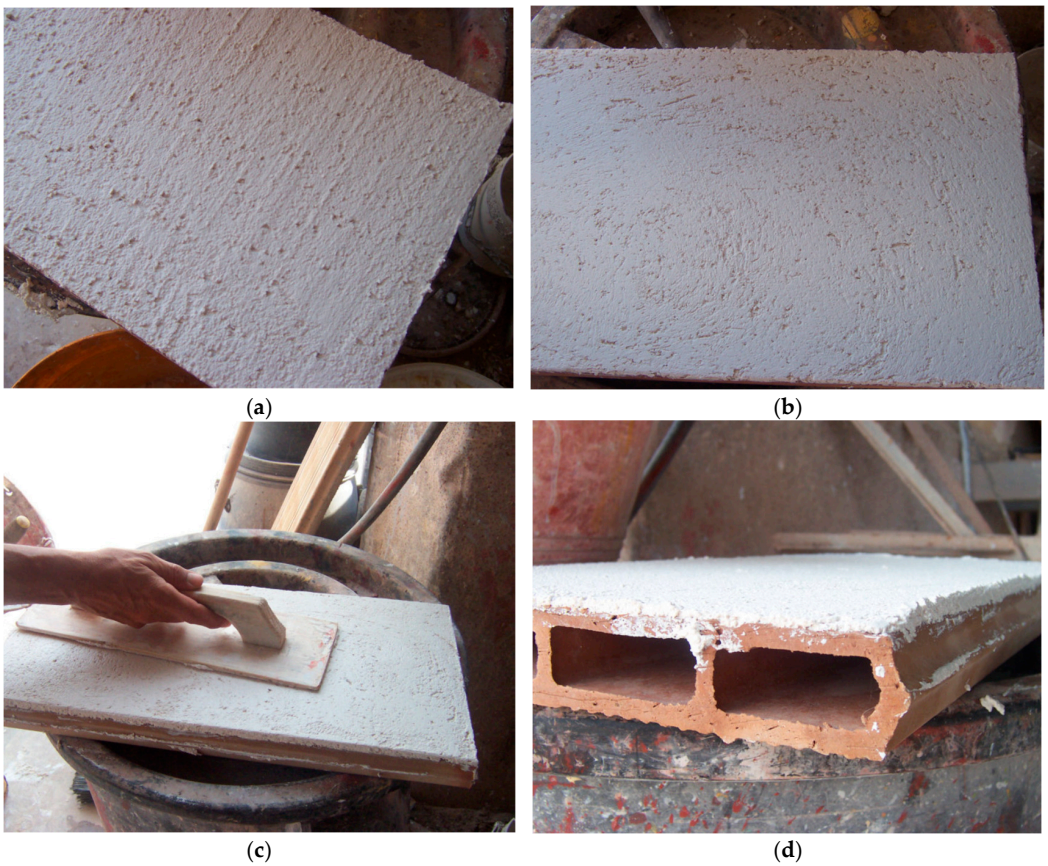

**Figure 10.** Applicability test of coarse plaster. First layer of mortar (**a**), Second layer of plaster (**b**), Surface treatment with the wooden trowel (**c**), 1 cm thick layer of plaster (**d**).

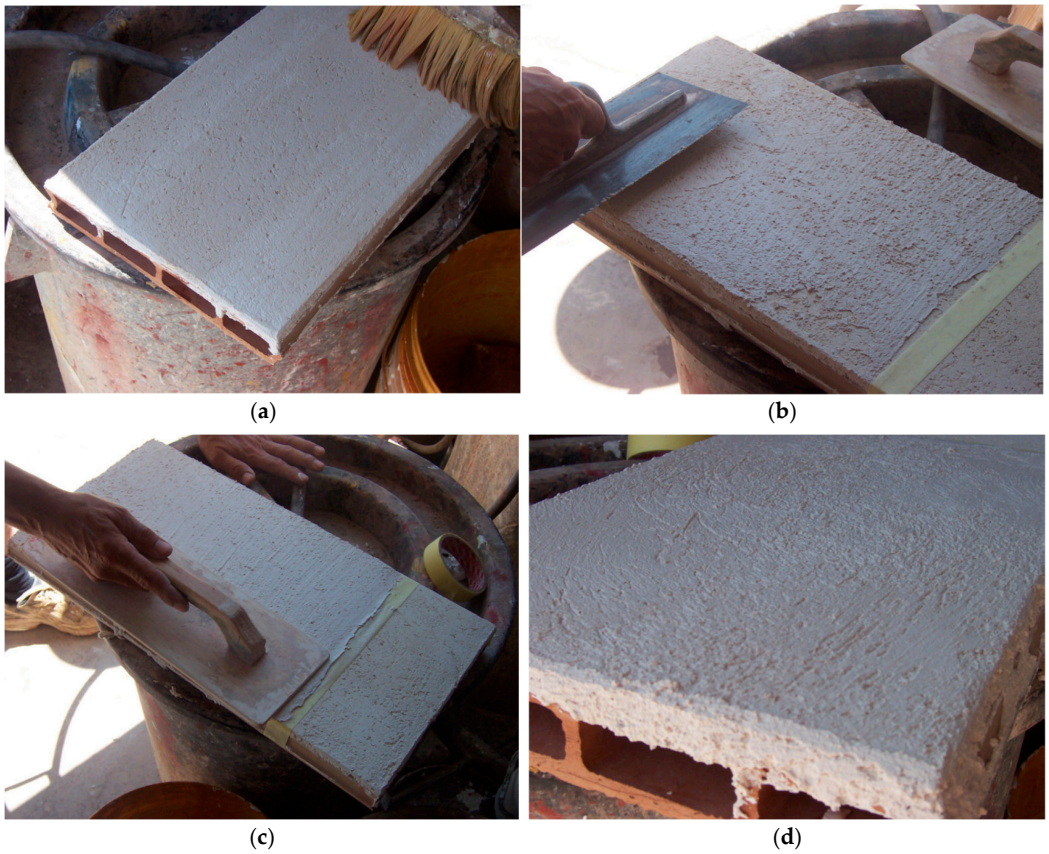

(**a**) (**b**)

(**c**) (**d**)

**Figure 11.** Applicability test of fine mortar. Coarse plaster wet with the brush (**a**), First layer of plaster applied with a steel trowel (**b**), Surface treatment with the wooden trowel (**c**), 1 cm thick layer of coarse plaster, and 2 mm thick layer of fine plaster (**d**).

(**a**) (**b**)

**Figure 12.** Applicability test of white fine mortar. First layer of finishing plaster applied with steel trowel (**a**), surface treatment with a small wooden trowel (**b**).

Fine plaster and finishing plaster were applied over the coarse plaster layer to a thickness of 2 mm and 1.5 mm, respectively. After thoroughly wetting the layer of hardened coarse plaster, the first coat of 1 mm of fine plaster was applied using a metal trowel. As the thickness of this first layer is very thin (approx. 1 mm), it starts setting very quickly. Once the first layer was set, the second one was applied, taking care to keep the layer of the total package equal to 2 mm. Finally, the surface is worked with the wooden trowel with circular movement to prepare it for the subsequent layers.

The finishing plaster was applied on the surface of the hardened and moistened coarse plaster in a single 1.5 mm layer. When it began to set, it was sponged with a special trowel,

which in this case was chosen smaller than the one previously used so that the surface remains only slightly rough.

The preliminary results obtained on fresh mixture samples showed that the coarse plaster is suitable for the use of base plaster (arriccio) up to a thickness of approximately 1 cm. For greater thicknesses, it must be applied in successive layers, waiting until the previous layer has been set. Fine plaster is suitable for use as a second layer (tonachino) for a total thickness of 2 mm. It is perfectly applied over a base made with coarse mortar, of which, similar in composition and compatible in grain size of aggregates, it is a natural completion, allowing for the creation, not of simple overlapping of distinct layers, the cause of possible detachment and swelling, but rather a single body that ensures durability and resistance to external agents. Finishing plaster can be applied and also treated on the surface in the desired manner, for a maximum thickness of 1.5 mm. Moreover, finishing plaster is suitable for lime paints in restorations or recoveries of ancient masonry requiring white color.

Finally, the stability of the mixtures was evaluated in a qualitative manner, observing any developments related to the appearance of cracks and detachments from the support, following the approach used by JF Gonzales-Sanchez [69] at different ages after application. The observations were conducted at one-day, two-day, one-week, one-month, and two-month intervals. For each observation, a report was made indicating the condition of the specimens as follows: C1 = severe cracking, C2 = evident cracking, C3 = moderate cracking, C4 = little or no cracking; [3] D1 = detachment in different zones, D2 = detachment in the edge for the samples, D3 = good adherence. The results of these observations are presented in Table 10, which demonstrates that no instances of detachment or cracking were observed in any of the three typologies throughout the entire observation period.

**Table 10.** Cracking assessment and adherence assessment.

| Type of Plaster | 1d [1] | 2d [1] | 1w [1] | 1m [1] | 2m [1] |
|---|---|---|---|---|---|
| Coarse Plaster | C4 [2] D3 [3] | C4 [2] D3 [3] | C4 [2] D3 [3] | C4 [2] D3 [3] | C4 [2] D3 [3] |
| Fine Plaster | C4 [2] D3 [3] | C4 [2] D3 [3] | C4 [2] D3 [3] | C4 [2] D3 [3] | C4 [2] D3 [3] |
| Finishing Plaster | C4 [2] D3 [3] | C4 [2] D3 [3] | C4 [2] D3 [3] | C4 [2] D3 [3] | C4 [2] D3 [3] |

[1] 1d = one day, 2d= two day, 1w = one week, 1m = one month, 2m = two months; [2] C4 = little or no cracking; [3] D3 = good adherence.

The absence of cracking can be attributed to the mix design and, in particular, to the inert component, which includes fine fractions such as SWS. The addition of this fraction allowed the formation of a stronger and more compact load-bearing skeleton with a lower presence of voids, which counteracts the shrinkage of the binder caused by both evaporation and carbonation of lime putty. The skeleton, with the presence of an extremely fine material, thus allows both good workability and excellent skeleton structure.

As mentioned above, while mix designs that involve replacing parts of the aggregates with SWS have been tested in the case of mortars in which the binder is cement, the authors found no scientific studies applying such a substitution in lime-based mortars. Therefore, it was not possible to make further comparative analyses with similar studies.

## 4. Conclusions

In this study, the possibility of producing mortars by introducing SWS into the mix as a substitute for aggregate in various proportions was investigated. A preliminary characterization of SWS was carried out.

Analyses were conducted to verify the mineralogical and chemical composition, the particle size distribution, and the ISO Brightness Level; the main conclusions are summarized below:

- The SWS consisted of 98.4% $CaCO_3$ by mass.
- The particle sizes are below 22.5 μm for the 92% by mass.
- ISO Brightness Level is 93.5% ± 1.

The results of the evaluation of the behavior of fresh plasters produced from lime putty, aged for 6 months, and from SWS partially replacing sand have proven to be extremely interesting as they provided a preliminary overview of the potential of the mortar, both in terms of workability and applicability of the plasters in the different subsequent layers. Therefore, this material has considerable potential for use as green material for plastering and finishing building surfaces in both new construction and historic heritage conservation. In the next phase, after the evaluation of the fresh behavior, which is particularly important for plasters and finishes, the mechanical characteristics, durability, and adhesion of the mixtures selected with the best fresh behavior will be evaluated. The mixtures have been designed using lime putties produced in a traditional way, using as fuel the wood waste produced in the immediate vicinity of the kiln, according to a good practice of industrial synergy. In addition, replacing natural aggregates with stone processing waste, the disposal of which is a major environmental issue, reduces the environmental impact. This applies both to the environmental impact caused by the disposal of the waste and to the environmental impact caused by the extraction of the otherwise necessary raw materials. However, a rigorous study entirely dedicated to the LCA is of fundamental importance and will be carried out in relation to further developments in research and the selection of mixtures with the best behavior in the fresh state.

**Author Contributions:** Conceptualization, G.B., F.F. and A.S.; methodology, A.S.; validation, G.B., F.F. and A.S.; investigation, A.S.; resources, G.B.; data curation, A.S. and G.B. and I.M.; writing—original draft preparation, A.S.; writing—review and editing, A.S. and G.B.; visualization, A.S.; supervision, F.F.; project administration, G.B.; funding acquisition, G.B. All authors have read and agreed to the published version of the manuscript.

**Funding:** This research was funded by MUR, grant number D.D. MUR 23 June 2022, n. 1049, identification code ECS00000009, CUP C43C22000400006, Research project "Tech4You-Technologies for climate change adaptation and quality of life improvement", Pilot Project 4.2.1 "Materials, architecture and design: open knowledge and innovative digital tools for cultural heritage", Action 2 "Nanoparticles for conservation".

**Institutional Review Board Statement:** Not applicable.

**Informed Consent Statement:** Not applicable.

**Data Availability Statement:** Data are contained within the article.

**Acknowledgments:** The authors would like to acknowledge Legnami Adriatica S.r.l. for supporting the production and testing of the specimens, Pietro Stefanizzi, for collaborating in the characterization of SWS, and Alessandra Pierucci for collaborating in the manufacturing of the specimens.

**Conflicts of Interest:** The authors declare no conflicts of interest.

## References

1. Elert, K.; Rodriguez-Navarro, C.; Pardo, E.S.; Hansen, E.; Cazalla, O. Lime Mortars for the Conservation of Historic Buildings. *Stud. Conserv.* **2002**, *47*, 62–75. [CrossRef]
2. Rattazzi, A. *Conosci il Grassello di Calce? Origine, Produzione e Impiego del Grassello di Calce in Architettura, Nell'arte e Nel Restauro*; Edicom: Gorizia, Italy, 2007.
3. Graziella, B.; Antonella, G. Heritages of stone: Materials degradation and restoration works. In Proceedings of the ReUSO 2015 III Congreso Internacional sobre Documentacion, Conservacion, y Reutilizacion del Patrimonio Arquitectonico y Paisajistico, Valencia, Spain, 22–24 October 2015; Editorial Universitat Politecnica de Valencia: Valencia, Spain, 2015; pp. 299–306.
4. Hansen, E.F.; Rodríguez-Navarro, C.; Balen, K. Lime Putties and Mortars. *Stud. Conserv.* **2008**, *53*, 9–23. [CrossRef]
5. Wu, C.; Huang, Q.; Xu, Z.; Sipra, A.T.; Gao, N.; de Souza Vandenberghe, L.P.; Vieira, S.; Soccol, C.R.; Zhao, R.; Deng, S.; et al. A comprehensive review of carbon capture science and technologies. *Carbon Capture Sci. Technol.* **2024**, *11*, 100178. [CrossRef]
6. Tian, S.; Jiang, J.; Zhang, Z.; Manovic, V. Inherent potential of steelmaking to contribute to decarbonisation targets via industrial carbon capture and storage. *Nat. Commun.* **2018**, *9*, 4422. [CrossRef] [PubMed]
7. Naeem, M.A.; Armutlulu, A.; Imtiaz, Q.; Donat, F.; Schäublin, R.; Kierzkowska, A.; Müller, C.R. Optimization of the structural characteristics of CaO and its effective stabilization yield high-capacity $CO_2$ sorbents. *Nat. Commun.* **2018**, *9*, 2408. [CrossRef]
8. Xu, Y.; Shen, C.; Lu, B.; Luo, C.; Wu, F.; Li, X.; Zhang, L. Study on the effect of NaBr modification on CaO-based sorbent for $CO_2$ capture and $SO_2$ capture. *Carbon Capture Sci. Technol.* **2021**, *1*, 100015. [CrossRef]

9. Rodriguez-Navarro, C.; Hansen, E.; Ginell, W.S. Calcium Hydroxide Crystal Evolution upon Aging of Lime Putty. *J. Am. Ceram. Soc.* **1998**, *81*, 3032–3034. [CrossRef]
10. Cazalla, O.; Rodriguez-Navarro, C.; Sebastian, E.; Cultrone, G.; De la Torre, M.J. Aging of lime putty: Effects on traditional lime mortar carbonation. *J. Am. Ceram. Soc.* **2000**, *83*, 1070–1076. [CrossRef]
11. Moropoulou, A.; Bakolas, A.; Bisbikou, K. Investigation of the technology of historic mortars. *J. Cult. Herit.* **2000**, *1*, 45–58. [CrossRef]
12. Moropoulou, A.; Bakolas, A.; Aggelakopoulou, E. The effects of limestone characteristics and calcination temperature to the reactivity of the quicklime. *Cem. Concr. Res.* **2001**, *31*, 633–639. [CrossRef]
13. Rodriguez-Navarro, C.; Ruiz-Agudo, E.; Ortega-Huertas, M.; Hansen, E. Nanostructure and irreversible colloidal behavior of $Ca(OH)_2$: Implications in cultural heritage conservation. *Langmuir* **2005**, *21*, 10948–10957. [CrossRef] [PubMed]
14. Ruiz-Agudo, E.; Rodriguez-Navarro, C. Microstructure and rheology of lime putty. *Langmuir* **2010**, *26*, 3868–3877. [CrossRef] [PubMed]
15. Mascolo, G.; Mascolo, M.C.; Vitale, A.; Marino, O. Microstructure evolution of lime putty upon aging. *J. Cryst. Growth* **2010**, *312*, 2363–2368. [CrossRef]
16. Paiva, H.; Velosa, A.; Veiga, R.; Ferreira, V.M. Ferreira, Effect of maturation time on the fresh and hardened properties of an air lime mortar. *Cem. Concr. Res.* **2010**, *40*, 447–451. [CrossRef]
17. Rosell, J.R.; Haurie, L.; Navarro, A.; Cantalapiedra, I.R. Influence of the traditional slaking process on the lime putty characteristics. *Constr. Build. Mater.* **2014**, *55*, 423–430. [CrossRef]
18. Bernardo, G.; Louis, P.I. Nanotech materials for the maintenance of the outer surfaces. In Proceedings of the Colloqui.AT.e, MATER(i)A, Materials/Architecture/Technology/Energy/Environment Reuse (Interdisciplinary)/Adaptability, Matera, Italy, 12–15 October 2016; Gangemi International: Rome, Italy, 2016; pp. 167–272.
19. Italian Trade Agency. XXX Rapporto Marmo e Pietre nel Mondo 2019-Nota di Mercato Settore Lapideo. Available online: https://www.ice.it/it/sites/default/files/inline-files/Nota%20di%20Mercato%20-%20Lapideo%20-%20June%202021.pdf. (accessed on 18 March 2024).
20. ISTAT. Annuario Statistico Italiano 2023-Cap 2-Ambiente, Clima ed Energia. Available online: https://www.istat.it/storage/ASI/2023/capitoli/C02.pdf (accessed on 27 March 2024).
21. N. 152 Decreto legislativo 3 Aprile 2006, Norme in Materia Ambientale (G.U. n. 88 del 14 aprile 2006). Available online: https://www.gazzettaufficiale.it/dettaglio/codici/materiaAmbientale (accessed on 18 March 2024).
22. Petruzzelli, D.; Petrella, M.; Boghetich, G.; Calabrese, P.; Petruzzelli, V.; Petrella, A. Neutralization of acidic wastewater by the use of waste limestone from the marble industry. Mechanistic aspects and mass transfer phenomena of the acid-base reaction at the liquid-solid interface. *Ind. Eng. Chem. Res.* **2009**, *48*, 399–405. [CrossRef]
23. Al-Zboon, K.K. Recycling of stone cutting waste for heavy metals removal. *J. Solid Waste Technol. Manag.* **2018**, *44*, 356–360. [CrossRef]
24. Regione Lazio-Direzione Regionale Ambiente. Osservatorio Ambientale Centrale Termoelettrica ENEL di Civitavecchia Torrevaldaliga Nord-Rapporto 2010. Available online: https://www.arpalazio.it/documents/20124/78596/AMB_PBL_Rapporto_Osservatorio_Ambientale_2010.pdf (accessed on 18 March 2024).
25. ENEL. Dichiarazione Ambientale Anni 2021–2024 Centrale Termoelettrica 'Andrea Palladio' di Fusina (VE) Via dei Cantieri, 5 Fusina (VE). Available online: https://corporate.enel.it/content/dam/enel-corporate/progetti/documenti/impianti-emas---termoelettrici/fusina/Dichiarazione_Ambientale_Aggiornamento_2023.pdf (accessed on 18 March 2024).
26. ENEL-Divisione Generazione ed Energy Management Unità di Business della Spezia, Relazione Tecnica dei Processi Produttivi-Centrale Eugenio Montale della Spezia. Available online: https://va.mite.gov.it/File/Documento/252005 (accessed on 18 March 2024).
27. Tozsin, G.; Oztas, T.; Arol, A.I.; Kalkan, E. Changes in the chemical composition of an acidic soil treated with marble quarry and marble cutting wastes. *Chemosphere* **2015**, *138*, 664. [CrossRef]
28. Tozsin, G.; Arol, A.I.; Oztas, T.; Kalkan, E. Using marble wastes as a soil amendment for acidic soil neutralization. *J. Environ. Manag.* **2014**, *133*, 374. [CrossRef]
29. Garas, G.L.; Allam, M.; Bakhoum, E.S. Studies Undertaken to Incorporate Marble and Granite Wastes in Green Concrete Production. *ARPN J. Eng. Appl. Sci.* **2014**, *9*, 1559–1564.
30. Jain, K.L.; Sancheti, G.; Gupta, L.K. Durability performance of waste granite and glass powder added concrete. *Constr. Build. Mater.* **2020**, *252*, 119075. [CrossRef]
31. Kore, S.D.; Vyas, A.K. Impact of marble waste as coarse aggregate on properties of lean cement concrete. *Case Stud. Constr. Mater.* **2016**, *4*, 85–92. [CrossRef]
32. Allam, M.E.; Bakhoum, E.S.; Ezz, H.; Garas, G.L. Influence of Using Granite Waste on the Mechanical Properties of Green Concrete. Available online: https://www.researchgate.net/publication/308670648 (accessed on 4 August 2024).
33. Allam, M.E.; Bakhoum, E.S.; Garas, G.L. Re-Use of Granite Sludge in Producing Green Concrete. 2014. Available online: https://www.researchgate.net/publication/287919960 (accessed on 4 August 2024).
34. Kumar, M.; Malay, N.; Kujur, J. Study of natural carbonation of concrete incorporating marble dust. *Proc. Inst. Civ. Eng. Constr. Mater.* **2018**, *171*, 85–92. [CrossRef]

35. Ince, C.; Hamza, A.; Derogar, S.; Ball, R.J. Utilisation of waste marble dust for improved durability and cost efficiency of pozzolanic concrete. *J. Clean. Prod.* **2020**, *270*, 122213. [CrossRef]
36. Ahmad, J.; Manan, A.; Ali, A.; Ihsan, T.; Zaid, O.; Ullah, R. Effects of Partially and Totally Substitution of Marble Waste as a Fine Aggregate on Workability and Mechanical Performance of Concrete. *J. Civ. Environ. Eng.* **2020**, *10*, 1–6.
37. Bhavya, B.S.; Reshma, T.V.; Sankalpasri, S.S. Comparative Study on Partial Replacement of Concrete by Waste Materials for Sustainable Development. *S-JPSET* **2010**, *10*, 40–48.
38. Singh, P. Comparative Study on Use of Waste Marble Powder as Partial Replacement in Concrete Mix. *Int. J. Res. Appl. Sci. Eng. Technol.* **2018**, *6*, 3211–3214. [CrossRef]
39. Singh, S.; Nagar, R.; Agrawal, V.; Rana, A.; Tiwari, A. Sustainable utilization of granite cutting waste in high strength concrete. *J. Clean. Prod.* **2016**, *116*, 223–235. [CrossRef]
40. Singh, S.; Nagar, R.; Agrawal, V. Performance of granite cutting waste concrete under adverse exposure conditions. *J. Clean. Prod.* **2016**, *127*, 172–182. [CrossRef]
41. Singh, S.; Khan, S.; Khandelwal, R.; Chugh, A.; Nagar, R. Performance of sustainable concrete containing granite cutting waste. *J. Clean. Prod.* **2016**, *119*, 86–98. [CrossRef]
42. Kore, S.D.; Vyas, A.K. Cost Effective Design of Sustainable Concrete Using Marble Waste as Coarse Aggregate. 2016. Available online: https://www.researchgate.net/publication/312128403 (accessed on 4 August 2024).
43. Kore, S.D.; Vyas, A.K. Behavior of Concrete Using Marble Waste as Coarse Aggregate. Available online: https://www.researchgate.net/publication/292149384 (accessed on 4 August 2024).
44. Nagaraj, H.B.; Anand, K.V.; Devaraj, N.C. Utilization of granite sludge in the preparation of durable compressed stabilized earth blocks. *MOJ Civ. Eng.* **2018**, *4*, 237–243. [CrossRef]
45. Ma, B.; Wang, J.; Tan, H.; Li, X.; Cai, L.; Zhou, Y.; Chu, Z. Utilization of waste marble powder in cement-based materials by incorporating nano silica. *Constr. Build. Mater.* **2019**, *211*, 139–149. [CrossRef]
46. Aydin, E.; Arel, H.Ş. High-volume marble substitution in cement-paste: Towards a better sustainability. *J. Clean. Prod.* **2019**, *237*, 117801. [CrossRef]
47. Mashaly, A.O.; Shalaby, B.N.; Rashwan, M.A. Performance of mortar and concrete incorporating granite sludge as cement replacement. *Constr. Build. Mater.* **2018**, *169*, 800–818. [CrossRef]
48. Marvila, M.T.; de Azevedo, A.R.; Alexandre, J.; Colorado, H.; Pereira Antunes, M.L.; Vieira, C.M. Circular economy in cementitious ceramics: Replacement of hydrated lime with a stoichiometric balanced combination of clay and marble waste. *Int. J. Appl. Ceram. Technol.* **2021**, *18*, 192–202. [CrossRef]
49. Alabsy, M.T.; Gouda, M.M.; Abbas, M.I.; Al-Balawi, S.M.; El-Khatib, A.M. Enhancing the Gamma-Radiation-Shielding Properties of Gypsum–Lime–Waste Marble Mortars by Incorporating Micro- and Nano-PbO Particles. *Materials* **2023**, *16*, 1577. [CrossRef]
50. Paes, A.L.; Alexandre, J.; Xavier, G.D.C.; Monteiro, S.N.; de Azevedo, A.R.G. Feasibility Analysis of Mortar Development with Ornamental Rock Waste for Coating Application by Mechanized Projection. *Sustainability* **2022**, *14*, 5101. [CrossRef]
51. Khyaliya, R.K.; Kabeer, K.S.A.; Vyas, A.K. Evaluation of strength and durability of lean mortar mixes containing marble waste. *Constr. Build. Mater.* **2017**, *147*, 598–607. [CrossRef]
52. Benjeddou, O.; Alyousef, R.; Mohammadhosseini, H.; Soussi, C.; Khadimallah, M.A.; Alabduljabbar, H.; Tahir, M.M. Utilisation of waste marble powder as low-cost cementing materials in the production of mortar. *J. Build. Eng.* **2020**, *32*, 101642. [CrossRef]
53. Li, L.G.; Huang, Z.H.; Tan, Y.P.; Kwan, A.K.H.; Liu, F. Use of marble dust as paste replacement for recycling waste and improving durability and dimensional stability of mortar. *Constr. Build. Mater.* **2018**, *166*, 423–432. [CrossRef]
54. Xi, Y.; Anastasiou, E.; Karozou, A.; Silvestri, S. Fresh and hardened properties of cement mortars using marble sludge fines and cement sludge fines. *Constr. Build. Mater.* **2019**, *220*, 142–148. [CrossRef]
55. Marvila, M.T.; Alexandre, J.; de Azevedo, A.R.; Zanelato, E.B. Evaluation of the use of marble waste in hydrated lime cement mortar based. *J. Mater. Cycles Waste Manag.* **2019**, *21*, 1250–1261. [CrossRef]
56. Amaral, L.F.; Delaqua, G.C.G.; Nicolite, M.; Marvila, M.T.; de Azevedo, A.R.; Alexandre, J.; Vieira, C.M.F.; Monteiro, S.N. Eco-friendly mortars with addition of ornamental stone waste-A mathematical model approach for granulometric optimization. *J. Clean. Prod.* **2020**, *248*, 119283. [CrossRef]
57. Xu, S.; Wang, J.; Jiang, Q.; Zhang, S. Study of natural hydraulic lime-based mortars prepared with masonry waste powder as aggregate and diatomite/fly ash as mineral admixtures. *J. Clean. Prod.* **2016**, *119*, 118–127. [CrossRef]
58. Megna, B.; Badagliacco, D.; Sanfilippo, C.; Valenza, A. Physical and mechanical properties of sustainable hydraulic mortar based on marble slurry with waste glass. *Recycling* **2021**, *6*, 37. [CrossRef]
59. *UNI 10802: 2023*; Rifiuti–Campionamento Manuale del Campione ed Analisi degli Eluati. ISO: Geneva, Switzerland, 2023. Available online: https://store.uni.com/uni-10802-2023 (accessed on 26 April 2024).
60. *UNI 8243:1981*; Prove sulle Materie Prime Non Fibrose per l'Industria Cartaria. Determinazione dell'Indice Riflettometrico Nel Blu (Grado di Bianco) delle Cariche Minerali e dei Pigmenti per Patina. ISO: Geneva, Switzerland, 1981. Available online: https://store.uni.com/uni-8243-1981 (accessed on 18 March 2024).
61. *UNI ISO 2470-1:2016*; Carta, Cartone e Paste-Misurazione del Fattore di Riflettanza Diffusa Nel Blu-Parte 1: Condizioni di Luce Diurna Interna (Grado di Bianco ISO). ISO: Geneva, Switzerland, 2016. Available online: https://store.uni.com/uni-iso-2470-1-2016 (accessed on 18 March 2024).

62. *UNI EN 196-6:2019*; Methods of Testing Cement-Part 6a Determination of Fineness (Blaine Method). ISO: Geneva, Switzerland, 2019. Available online: https://store.uni.com/uni-en-196-6-2019 (accessed on 18 March 2024).
63. *UNI EN 1015-3:2007*; Test Methods for Mortar for Masonry Work. ISO: Geneva, Switzerland, 2007. Available online: https://store.uni.com/uni-en-1015-3-2007 (accessed on 18 March 2024).
64. Zacharopoulou, G. The renascence of lime based mortar technology an appraisal of a bibliographic study. *Compat. Mater. Prot. Eur. Cult. Herit.* **1988**, *55*, 89–114.
65. Van Balen, K. Understanding the lime cycle and its influence on historical construction practice. In Proceedings of the First International Congress on Construction History, Madrid, Spain, 20–24 January 2003.
66. N. 186 Decreto Ministeriale 5 Aprile 2006. *Regolamento Recante Modifiche al Decreto Ministeriale 5 Febbraio 1998 «Individuazione dei Rifiuti Non Pericolosi Sottoposti alle Procedure Semplificate di Recupero, ai Sensi degli Articoli 31 e 33 del Decreto Legislativo 5 Febbraio 1997, n. 22.* Available online: https://www.gazzettaufficiale.it/eli/id/2006/05/19/006G0202/sg (accessed on 18 April 2024).
67. Associazione Geotecnica Italiana (AGI). Nomenclatura Geotecnica e Classifica delle Terre. Available online: https://associazionegeotecnica.it/articoli_rig/nomenclatura-geotecnica-e-classifica-delle-terre (accessed on 18 March 2024).
68. González-Fonteboa, B.; González-Taboada, I.; Carro-López, D.; Martínez-Abella, F. Influence of the mixing procedure on the fresh state behaviour of recycled mortars. *Constr. Build. Mater.* **2021**, *299*, 124266. [CrossRef]
69. Gonzalez-Sanchez, J.F.; Fernández, J.M.; Navarro-Blasco, Í.; Alvarez, J.I. Improving lime-based rendering mortars with admixtures. *Constr. Build. Mater.* **2021**, *271*, 121877. [CrossRef]